INTERNATIONAL JOURNAL FOR NUMERICAL AND ANALYTICAL METHODS IN GEOMECHANICS, VOL. 21, 507–532 (1997)

VERTICALLY LOADED PILES IN NON-HOMOGENEOUS MEDIA

WEI DONG GUO* AND MARK F. RANDOLPH

Geomechanics Group, Department of Civil Engineering, University of Western Australia, Nedlands, WA 6907, Australia

SUMMARY

Analytical methods for the axial responses of piles can be classified under three broad categories of (1) simple but approximate analytical solutions, (2) one-dimensional numerical algorithms, (3) full axisymmetric analyses using boundary or finite element approaches. The first two categories rely on the so-called load transfer approach, with interaction between pile and soil determined by independent springs distributed along the pile shaft and at the pile base. The non-linear spring stiffness is related to the elastic–plastic properties of the actual soil partly by empirically based correlations and partly by theoretical arguments based on simplified models of the pile–soil system. This paper presents new closed-form solutions for the axial response of piles in elastic–plastic, non-homogeneous, media. The solutions fall in the first of the three categories above, and have been verified through extensive parametric studies using more rigorous one-dimensional and continuum analyses. The effect of non-homogeneity and partial slip on the load and displacement profiles along the pile shaft is explored, and comparisons are presented with experimental data.

Int. J. Numer. Anal. Meth. Geomech., Vol. 21, 507–532 (1997)
(No. of Figures: 16 No. of Tables: 0 No. of Refs: 22)

Key words: piles; axial loading; closed-form solutions; non-homogeneous; non-linear

INTRODUCTION

The load-settlement response of single piles and pile groups is significantly affected by non-homogeneity in stiffness and strength of the ground. Three aspects of the response may be identified: (a) the pile-head settlement at working load; (b) the distribution of load down the pile; and (c) the degree of the interaction between piles within a group. While, for piles of moderate slenderness ratio, the settlement under working load is primarily a function of the average stiffness of the ground over the depth of embedment of the pile, variations in stiffness and limiting shaft friction with depth have an increasing influence as the slenderness of the pile increase. For all piles, however, the relative homogeneity of the soil is critical in determining the load distribution along the pile and also interaction between piles.

Analytical methods for piles fall into two main categories: continuum-based, such as the boundary or finite element methods, or load transfer approaches. The latter category quantifies interaction between pile and soil through a series of independent springs distributed along the pile and at the base.[1] For pile groups and piled rafts, increasing use is being made of a so-called

*Correspondence to W. D. Guo, Geomechanics Group, Department of Civil Engineering, University of Western Australia, Nedlands, WA 6907, Australia.

CCC 0363–9061/97/080507–26$17.50

Received 9 August 1996
Revised 18 November 1996

'hybrid' approach, where load transfer springs are used to obtain the response of each single pile, while a continuum model is used to assess effects of interaction between different piles and with the pile cap or raft.[2,3]

The load transfer approach is attractive in its flexibility, enabling non-linear and heterogeneous soil conditions to be incorporated easily. At the other extreme, closed-form solutions may be obtained for homogeneous elastic-perfectly plastic load transfer spring stiffness,[4–6] which may also be related to the elastic properties of the soil in order to simulate continuum-based solutions.[7]

The present paper addresses the response of axially loaded piles in a generic non-homogeneous soil where stiffness and strength vary monotonically with depth. The main aims of the paper are:

(1) to calibrate the relationship between load transfer spring stiffness and elastic soil properties, extending the work of Randolph and Wroth[7] to consider the effect of non-homogeneity on the relationship;
(2) to present new closed-form solutions for the case of elastic-perfectly plastic soil response with stiffness and strength varying as a power law of depth.
(3) to develop a spreadsheet program called GASPILE, which is then adopted to explore the difference between non-linear elastic–plastic and elastic–perfectly plastic analyses.

The study uses continuum analyses from previous published work, and from an extensive parametric study undertaken using the finite-difference program, FLAC,[8] to verify the closed-form solutions. The solutions are also used to back-analyse field data, allowing comparison of computed and measured load distributions.

LOAD TRANSFER MODELS

Expressions of non-homogeneity

The soil profile concerned and the relevant non-dimensional parameters adopted in this paper are briefly described below.

(1) The initial soil shear modulus (G_i) distribution down a pile is assumed as a power function of depth[9]

$$G_i = A_g z^n \tag{1}$$

where A_g and n are constants and z is the depth below the ground surface. The average shear modulus down the pile can be estimated by

$$G_{ave} = A_g L^n/(n+1) \tag{2}$$

where L is the pile embedded length. Below the pile tip level, the shear modulus is kept as a constant, G_{ib}. Therefore, the pile base shear modulus jump is expressed by the ratio, $\xi_b (= G_{iL}/G_{ib})$, where G_{iL} is shear modulus just above the pile base level; ξ_b is referred to as the end-bearing factor, which is assumed to be unity in this paper except where specified. Figure 1 shows examples of the shear modulus distribution.

(2) Generally, it is assumed that the ratio of the limiting shaft friction to shear modulus falls into a narrow range,[7] particularly for a given soil and pile combination. The limiting shaft friction may be expressed, in a similar manner to the shear modulus, as

$$\tau_f = A_v z^\theta \tag{3}$$

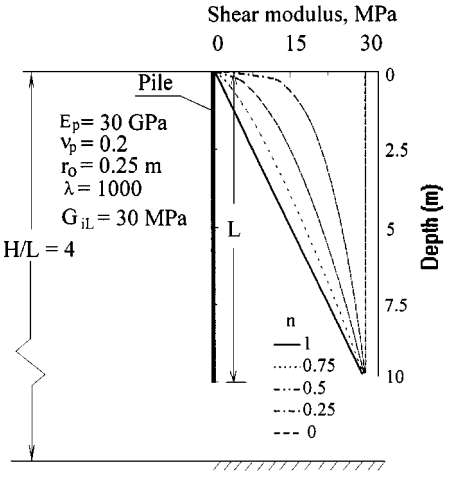

Underlying rigid layer simulated by constraining the vertical displacement

Figure 1. Example pile–soil system for FLAC analysis

where A_v and θ are constants. In this paper, attention will be restricted to the case of n being equal to θ. Therefore, the ratio of modulus to limiting shaft stress is invariant with the depth, and is equal to A_g/A_v.

(3) Non-homogeneity factor is expressed by (a) $\rho_g = G_{ave}/G_{iL} = 1/(n+1)$, which was referred to as the shaft non-homogeneity factor;[7] (b) $\eta = G_{io}/G_{iL}$ by Poulos,[10] where G_{io} is the shear modulus at the mudline level. This definition is suitable for a Gibson soil, in which the soil modulus increases linearly with depth; or (c) simply by the power n.

(4) Pile–soil relative stiffness ratio may be expressed as (a) the ratio of pile Young's modulus, E_p, and the base level soil Young's modulus, E_{iL}, by Poulos,[10] i.e.

$$K_b = E_p/E_{iL} \tag{4}$$

or (b) the ratio of E_p, to the shear modulus at pile base level, G_{iL}, by Randolph and Wroth,[7] i.e.

$$\lambda = E_p/G_{iL} \tag{5}$$

As discussed by Guo,[11] the non-homogeneity factor n, and the relative stiffness factor λ are adopted in the current research. For ease of comparison, the previously published results will be converted and expressed in terms of these non-dimensional parameters later.

Elastic stiffness

Theoretical load transfer models were developed for a homogeneous or Gibson soil,[7] where the stiffness of the load transfer relationship for soil along the pile shaft and at the pile base was expressed in terms of the elastic properties of the soil. These models are extended further to more general non-homogeneous soil profile as described below.

Shaft load transfer model. The shaft displacement, w, is related to the local shaft stress, τ_0, and initial shear modulus, G_i, by Randolph and Wroth:[7]

$$w = \frac{\tau_0 r_0}{G_i}\zeta \tag{6}$$

where r_0 is the radius of the pile and ζ is a parameter given by

$$\zeta = \ln\left(\frac{r_m}{r_0}\right) \tag{7}$$

where the parameter, r_m, represents the maximum radius of influence of the pile beyond which the shear stress becomes negligible, and is discussed further below. Using a hyperbolic law to model the soil stress–strain relationship, the parameter ζ can then be expressed as [12,13]

$$\zeta = \ln\left[\left(\frac{r_m}{r_0} - \psi_0\right)\Big/(1 - \psi_0)\right] \tag{8}$$

where the term, $\psi_0 (= R_{fs}\tau_0/\tau_f)$, represents the non-linear stress level at the pile–soil interface (the limiting stress being assumed to be equal to the failure shaft stress); R_{fs} is a parameter controlling the degree of non-linearity.

The critical value of the maximum radius of influence of the pile beyond which the shear stress becomes negligible was expressed in terms of the pile length, L, as[7]

$$r_m = 2{\cdot}5\rho_g(1 - \nu_s)L \tag{9}$$

where ν_s is the Poisson ratio. This estimation of r_m is generally valid for a pile embedded in an infinite layer. More generally, it can be expressed as

$$r_m = A\frac{1 - \nu_s}{1 + n}L + Br_0 \tag{10}$$

Values of A and B for different pile geometry, pile–soil stiffness, and various thickness of finite soil layer are explored by the authors[14] and further in the thesis by Guo.[11]

The purpose of this paper is to establish closed-form solutions, using the load transfer approach. The assessment of the load transfer method, and the suitability of equation (10) are explained in detail in the thesis by Guo,[11] where it is shown that the load transfer factor, ζ can be taken as approximately constant with depth.

As the pile-head load increases, the mobilized shaft shear stress will reach the limiting value (τ_f). The local limiting displacement can be expressed as

$$w_e = \zeta r_0 \frac{A_v}{A_g} \tag{11}$$

Thereafter, as the pile–soil relative displacement exceeds the limiting value, the shear stress is kept as τ_f (i.e. an ideal elastic–perfectly plastic load transfer response is assumed). Due to the assumed similarity of the limiting shaft stress and the shear modulus distribution, the limiting shaft displacement is a constant down the pile.

The load transfer response may be taken as elastic, by assuming a constant value of ψ_0, (referred to as 'simple linear analysis (SL)'). Alternatively, non-linearity may be incorporated, expressing the parameter ψ_0 as a function of stress level and the constant R_{fs} in equation (8)

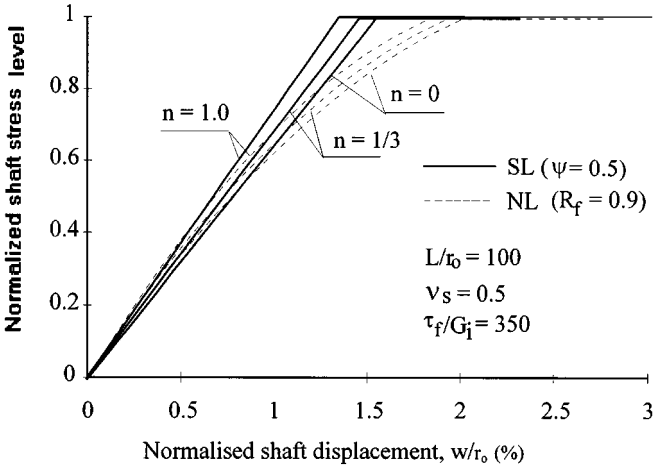

Figure 2. Comparison of load transfer behaviour estimated by non-linear and simple elastic–plastic approaches

(hence, ζ is dependent on stress level). This is referred to as non-linear (NL) analysis. As an example, Figure 2 shows the non-dimensional shear stress versus displacement relationship for NL ($R_{fs} = 0{\cdot}9$) and SL (ζ = constant with $\psi_0 = 0{\cdot}5$) analyses, with $\tau_f/G_i = 350$, $L/r_0 = 100$, and $\nu_s = 0{\cdot}5$. Note that full mobilization of shaft friction occurs at a displacement of 1–2% of the pile radius, which accords with experimental evidence.[15]

Base pile–soil interaction model. The base settlement can be estimated through the solution for a rigid punch acting on an elastic half-space, as suggested by Randolph and Wroth:[7]

$$w_b = \frac{P_b(1 - \nu_s)\omega}{4r_0 G_{ib}} \tag{12}$$

where P_b is the mobilized base load, ω is the pile base shape and depth factor which is generally chosen as unity.[7,16] This parameter has been assessed in detail in the thesis by Guo.[11] Using a hyperbolic model, the base load–displacement relationship can be given by[2]

$$w_b = \frac{P_b(1 - \nu_s)\omega}{4r_0 G_{ib}} \frac{1}{(1 - R_{fb}P_b/P_{fb})^2} \tag{13}$$

where P_{fb} is the limiting base load and R_{fb} is a parameter controlling the degree of non-linearity.

OVERALL PILE–SOIL INTERACTION

Generally, a pile is assumed to behave elastically, with constant diameter and Young's modulus. Therefore, the governing equation for pile–soil interaction can be written as[7]

$$\frac{d^2u(z)}{d^2z} = \frac{\pi d\tau_0}{E_p A_p} \tag{14}$$

where E_p and A_p are the Young's modulus and cross-sectional area of an equivalent solid cylinder pile, respectively, and $u(z)$ is the axial pile deformation.

Elastic solution

Within the elastic stage, the shaft stress in equation (14) can be expressed by the local displacement as prescribed by equation (6), in which the load transfer factor, ζ, is estimated by equation (8) with $\psi_0 = 0$. Therefore, the basic differential equation governing the axial deformation of a pile fully embedded in the non-homogeneous soil described by equation (1) is found to be

$$\frac{\mathrm{d}^2u(z)}{\mathrm{d}^2z} = \frac{A_\mathrm{g}}{E_\mathrm{p}A_\mathrm{p}}\frac{2\pi}{\zeta}z^n w(z) \tag{15}$$

The axial pile displacement, $u(z)$, should equal the pile–soil relative displacement, $w(z)$, when ignoring any external soil subsidence. Normally, the load transfer factor ζ can be taken as a constant along a pile depth.[7] Therefore, equation (15) can be solved in terms of modified Bessel functions of non-integer order

$$w(z) = \left(\frac{z}{L}\right)^{1/2}(A_1 I_m(y) + B_1 K_m(y)) \tag{16}$$

$$\frac{\mathrm{d}w(z)}{\mathrm{d}z} = -\frac{P(z)}{E_\mathrm{p}A_\mathrm{p}} = k_\mathrm{s}\left(\frac{z}{L}\right)^{1/2} z^{n/2}(A_1 I_{m-1}(y) - B_1 K_{m-1}(y)) \tag{17}$$

where $w(z)$ and $P(z)$ are the displacement and load at a depth of $z(0 < z \leqslant L)$, respectively, and $m = 1/(n+2)$. The variable y is

$$y = 2m\frac{L}{r_0}\sqrt{\frac{2}{\lambda\zeta}}\left(\frac{z}{L}\right)^{1/2m} \tag{18}$$

and the stiffness factor k_s,

$$k_\mathrm{s} = \frac{L}{r_0}\sqrt{\frac{2}{\lambda\zeta}}\left(\frac{1}{L}\right)^{1/2m} \tag{19}$$

The constants A_1 and B_1 can be found in terms of the stress and deformation compatibility conditions at the pile base,

$$w(L) = w_\mathrm{b} \tag{20}$$

$$\left[\frac{\partial w}{\partial z}\right]_{z=L} = -\frac{P_\mathrm{b}}{A_\mathrm{p}E_\mathrm{p}} = -\frac{4}{(1-\nu_\mathrm{s})\omega\pi}\frac{1}{\xi_\mathrm{b}\lambda}\frac{w_\mathrm{b}}{r_0} \tag{21}$$

where P_b has been expressed in terms of w_b, by equation (12). Therefore, the coefficients A_1, B_1 can be expressed, respectively, as

$$A_1 = w_\mathrm{b}(K_{m-1} - \chi_\mathrm{v}K_m)/(K_{m-1}I_m + \chi_\mathrm{v}K_m I_{m-1}) \tag{22}$$

$$B_1 = w_\mathrm{b}(I_{m-1} - \chi_\mathrm{v}I_m)/(K_{m-1}I_m + \chi_\mathrm{v}K_m I_{m-1}) \tag{23}$$

where I_m, I_{m-1}, K_{m-1} and K_m are the values of the modified Bessel functions for $z = L$. The ratio χ_v is given by

$$\chi_\mathrm{v} = \frac{P_\mathrm{b}}{w_\mathrm{b}}\frac{L}{E_\mathrm{p}A_\mathrm{p}}\Big/(k_\mathrm{s}L^{n/2+1}) = \frac{2\sqrt{2}}{\pi(1-\nu_\mathrm{s})\omega\xi_\mathrm{b}}\sqrt{\frac{\zeta}{\lambda}} \tag{24}$$

Substituting the expressions for A_1 and B_1 into equations (16) and (17), the displacement and load at any depth of z can be expressed, respectively, as

$$w(z) = w_b \left(\frac{z}{L}\right)^{1/2} \left(\frac{C_3(z) + \chi_v C_4(z)}{C_3(L)}\right) \tag{25}$$

$$P(z) = k_s E_p A_p w_b z^{n/2} \left(\frac{z}{L}\right)^{1/2} \left(\frac{C_1(z) + \chi_v C_2(z)}{C_3(L)}\right) \tag{26}$$

where

$$\begin{aligned} C_1(z) &= -K_{m-1} I_{m-1}(y) + K_{m-1}(y) I_{m-1} \\ C_2(z) &= K_m I_{m-1}(y) + K_{m-1}(y) I_m \\ C_3(z) &= K_{m-1} I_m(y) + K_m(y) I_{m-1} \\ C_4(z) &= -K_m I_m(y) + K_m(y) I_m \end{aligned} \tag{27}$$

At any depth z, the stiffness can be derived as

$$\frac{P(z)}{G_{iL} w(z) r_0} = \sqrt{2}\pi \sqrt{\frac{\lambda}{\zeta}} C_v(z) \tag{28}$$

where

$$C_v(z) = \frac{C_1(z) + \chi_v C_2(z)}{C_3(z) + \chi_v C_4(z)} \left(\frac{z}{L}\right)^{n/2} \tag{29}$$

At the ground surface, where $z = 0$, it is necessary to take the limiting value of $C_v(z)$ as z approaches zero. This will be referred to as C_{vo}. From equations (25) and (26), the base settlement can be written as a function of pile load and displacement as well. The accuracy of these closed-form solutions (CF) have been checked by using Mathcad™. Further corroboration by continuum-based finite-difference analysis is shown later.

Elastic–plastic solution

As the pile-head load increases, pile–soil relative slip is assumed to commence from the ground level and at any stage during loading may be taken to have developed to a depth called transition depth (L_1), at which the shaft displacement, w, corresponds to the local limiting displacement. The upper part of the pile, above the transition depth, is in a plastic state, while the lower part below this depth is in an elastic state. Within the plastic state, the shaft shear stress in equation (14) should be replaced by the limiting shaft stress equation (3). Pile-head load and settlement are, therefore, expressed, respectively, as a sum of the elastic part represented by letters with subscript of 'e', and the plastic part:

$$P_t = P_e + \frac{2\pi r_0 A_v L_1^{\theta+1}}{\theta + 1} \tag{30}$$

$$w_t = w_e + \frac{L_1}{E_p A_p} \left(\frac{2\pi r_0 A_v L_1^{1+\theta}}{1 + \theta} + P_e\right) \tag{31}$$

where $\mu = L_1/L$ is defined as the degree of slip ($0 < \mu \leqslant 1$), $L_1 + L_2 = L$ and L_2 is the length of the lower elastic part, which equals $L(1 - \mu)$. The pile load at the transition depth is written as P_e. Since $w(z) = w_e$ at the transition depth of L_1, $P_e = P(L_1)$ can be readily estimated from equation (28); therefore, equation (30) can be rewritten as

$$P_t = w_e k_s E_p A_p L^{n/2} C_v(\mu L) + \frac{2\pi r_0 A_v (\mu L)^{1+\theta}}{1+\theta} \tag{32}$$

Similarly, as a result of equation (31), and substituting for P_e, the pile–head settlement is expressed as

$$w_t = w_e[1 + \mu k_s L^{n/2+1} C_v(\mu L)] + \frac{2\pi r_0 A_v}{E_p A_p} \frac{(\mu L)^{2+\theta}}{2+\theta}. \tag{33}$$

These solutions provide three important results as shown below:

(1) For a given degree of slip, the pile-head load and settlement can be estimated by equations (32) and (33), respectively; therefore the full pile-head load-settlement relationship may be obtained.
(2) For a given pile-head load, the corresponding degree of slip of the pile can be back-figured by equation (32).
(3) The distribution profile of either load or displacement can be readily obtained, at any stage of the elastic–plastic development. Within the upper plastic part, at any depth of z:

   (i) from equation (30), the load, $P(z)$ can be predicted by

$$P(z) = P_e + 2\pi r_0 A_v \frac{(\mu L)^{\theta+1} - z^{1+\theta}}{\theta+1} \tag{34}$$

   (ii) from equation (31), the displacement, $w(z)$ can be obtained by

$$w(z) = w_e + \frac{P_e(\mu L - z)}{E_p A_p} + \frac{2\pi r_0 A_v}{E_p A_p}\left(\frac{z^{2+\theta} - (2+\theta) z (\mu L)^{\theta+1} + (1+\theta)(\mu L)^{2+\theta}}{(1+\theta)(2+\theta)}\right) \tag{35}$$

The current analysis is limited to the case of $n = \theta$, but the physical implications of n (related to elastic stage) and θ (to plastic stage) are completely different; therefore, both parameters are presevered in the equations.

PILE RESPONSE WITH HYPERBOLIC SOIL MODEL

A program for non-linear load transfer analysis

A program operating in Windows EXCEL called GASPILE has been developed to allow analysis of pile response in non-linear soil. The analytical procedure is similar to that proposed by Coyle and Reese[1] for computing load-settlement curves of a single pile under axial load. The pile is discretized into elements, each of which is connected to a soil load transfer spring. The load transferred is divided into two parts: the shaft where equation (6) is adopted, and the base where equation (13) is employed. The input parameters include (1) limiting pile–soil friction distribution

down the pile; (2) initial shear modulus distribution down the pile; (3) the end-bearing factor and soil Poisson's ratio; and (4) the dimensions and Young's modulus of the pile. Comparison[11] shows that the result from GASPILE are consistent with those from RATZ.[17]

To explore the effect of non-linear soil model, GASPILE has been used to analyse a typical pile–soil system: The pile is assumed to have dimensions of $L = 25$ m, $r_0 = 0{\cdot}25$ m and $E_p = 2{\cdot}9$ GPa, in a soil of $G_{ave} = 20$ MPa, Poisson's ratio, $\nu_s = 0{\cdot}4$; the ratio of modulus and strength, $G_i/\tau_f = 350$. The end-bearing factor has been taken as $\xi_b = 1$ and the ultimate base load as $P_{fb} = 1{\cdot}2$ MN. The pile is discretized into 20 segments, although in practice the results are very similar to those using 10 segments.

Shaft stress–strain non-linearity effect

GASPILE analyses has been performed, respectively, by using both the non-linear model (NL, R_{fs} = constant) model and the simple linear model (SL, ψ_0 = constant) as described previously and shown in Figure 2. To explore the difference in the shaft component of the pile response between the analyses using NL and SL models, identical base soil models have been adopted for both analyses, using hyperbolic model with R_{fb} of 0·9. Figure 3 shows that the analyses from the NL ($R_{fs} = 0{\cdot}9$) and SL ($\psi_0 = 0{\cdot}5$) models are generally consistent for (1) non-dimensional load and displacement distribution down the pile (two different base displacement, $w_b = 1{\cdot}5$, $3{\cdot}0$ are provided), and (2) the pile-head response (note that base behaviour is identical). This is probably because the shaft NL and SL models, as illustrated in Figure 2, are generally consistent with each other for stress levels below about 0·6–0·7. The difference in load transfer due to the variation of the degree of non-homogeneity can be sufficiently reflected by the simplified model (SL). For most realistic cases, the effect of non-linearity is expected to be significant only at load levels close to failure (e.g. Figure 3(c) for which $R_{fs} = 0{\cdot}9$). Therefore, it is generally sufficient to use the simplified model (SL) resulting in a constant value of ζ.

Base stress–strain non-linearity effect

The influence of base stress level is obvious only when a significant settlement occurs.[18] If the base settlement, w_b, is less than the local limiting displacement, w_e, the base soil is generally expected to behave elastically except when the underlying soil is less stiff than the soil above the pile base level ($\xi_b > 1$). However, in the case of $\xi_b > 1$, the base contribution becomes less important. Therefore, an elastic consideration of the base interaction before full shaft slip is generally adequate.

The effect of the non-linear stress–strain relationship on pile-head response is further illustrated in Figure 4 for soil of different profiles, with the result presented separately for clarity. Each presentation provides the comparison between closed-form solutions with two constant values of $\psi_0 = 0$, 0·5 and the NL ($R_{fs} = 0{\cdot}9$) analyses by GASPILE.

VERIFICATION OF THE THEORY

To verify the elastic solutions outline previously, a continuum-based numerical analysis was performed with the finite-difference program FLAC,[8] while the elastic–plastic solutions were substantiated by the available continuum-based solutions.[18,19]

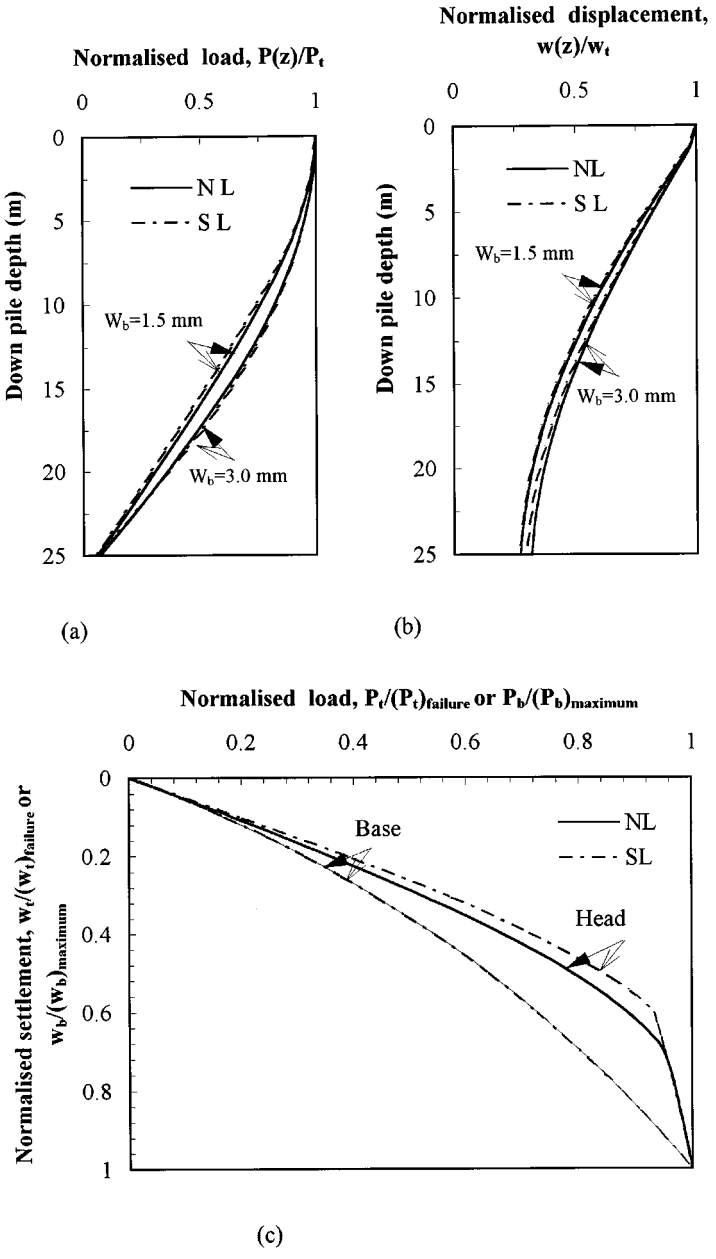

Figure 3. Comparison of pile load and displacement behaviour between the non-linear (NL) and linear (SL) analyses ($L/r_0 = 100$): (a) load distribution; (b) displacement distribution; (c) load settlement

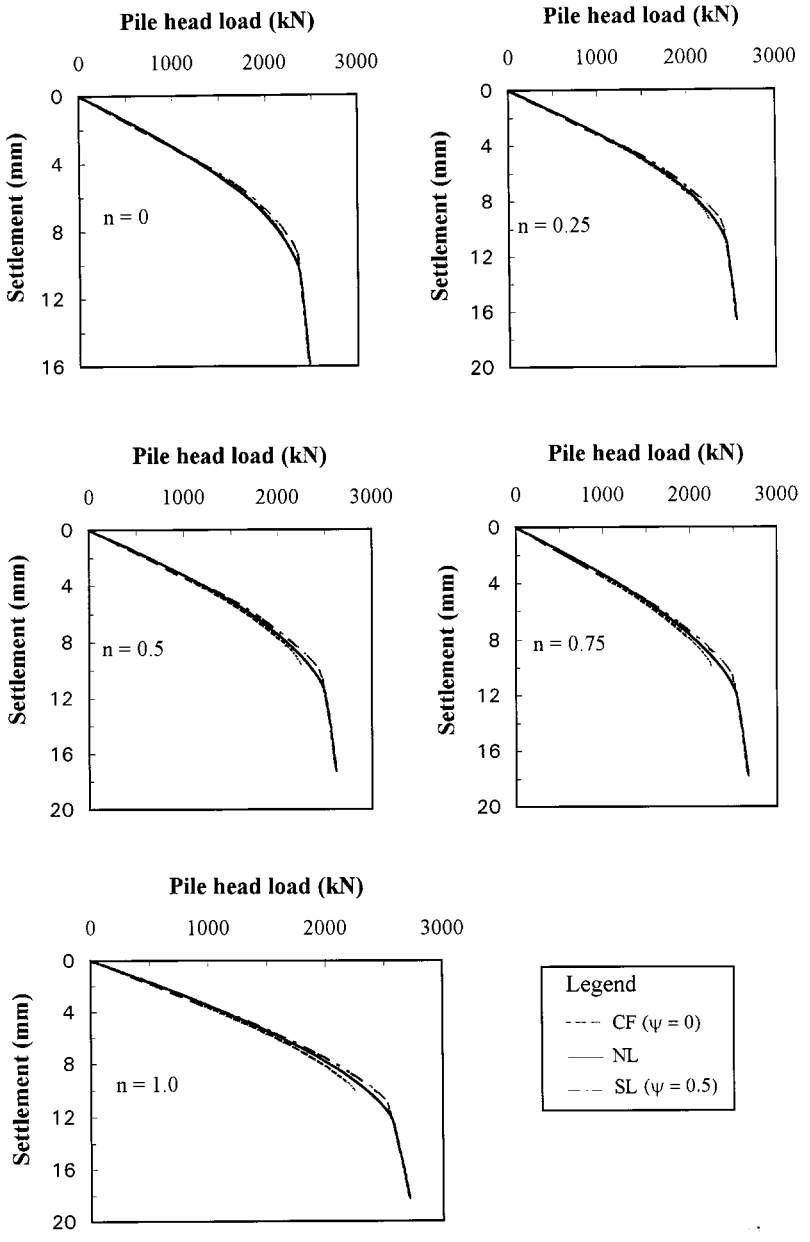

Figure 4. Comparison of pile–head load–settlement relationship among the non-linear and simple linear ($\psi = 0{\cdot}5$) GASPILE analyses and the CF solution ($L/r_0 = 100$)

FLAC analysis

For the current FLAC analysis, a typical axisymmetric grid generated is shown in Figure 5. The width of the grid was the maximum of $2{\cdot}5L$ and $75r_0$. The effect of the ratio of the depth to the underlying rigid layer, H, and the pile length, L, has been explored. As demonstrated in Figure 6, a decrease in H/L generally leads to an increase in the pile-head stiffness, particularly for the case of higher relative pile–soil stiffness. However, the difference becomes negligible, when the value of H/L exceeds 4. Therefore, in the following analysis, H is kept at $4L$ ($H/L = 4$) to minimize the boundary effect. In addition, Poisson's ratio of the pile has been taken as $\nu_p = 0{\cdot}2$.

Pile-head stiffness and settlement ratio

The closed-form solution for the pile response, which is later referred to as CF, depends on the load transfer parameter, ζ, which in turn depends on ψ_0 and r_m. The solutions presented below have been based on values of $A = 2$, $B = 0$, $\nu_s = 0{\cdot}4$, $\xi_b = 1$, $\psi_0 = 0$ and $\omega = 1$. Note that these values will be adopted in all the following analyses, except where specified. Justification for the choice of A and B has been presented by Guo.[11]

The pile-head stiffness predicted by equation (28) has been plotted against the result from FLAC analyses in Figure 7. The head stiffness obtained by the simple analysis (SA)[7] has been shown as well, albeit with $A = 2{\cdot}5$ (other parameters being identical to those adopted in equation (28)). The results show that:

(1) The CF approach is reasonably accurate but generally slightly underestimates the stiffness in comparison with the FLAC results. However the difference is less than 10 per cent.

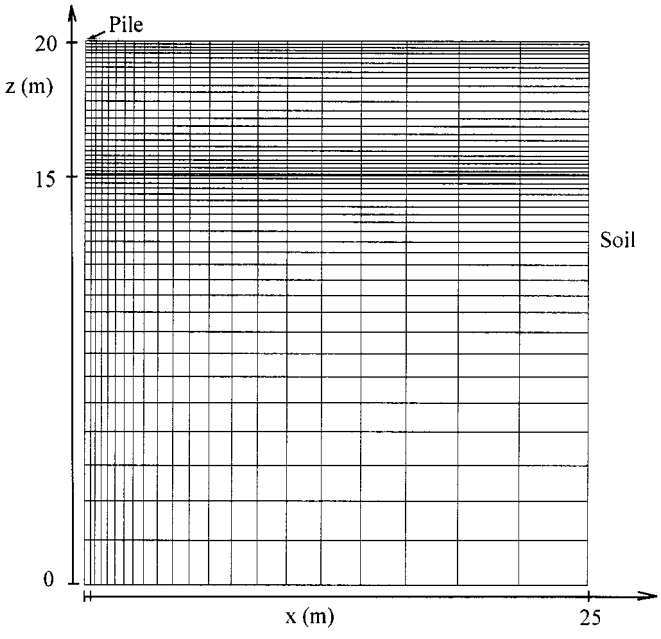

Figure 5. An example mesh for FLAC analysis ($L/r_0 = 20$)

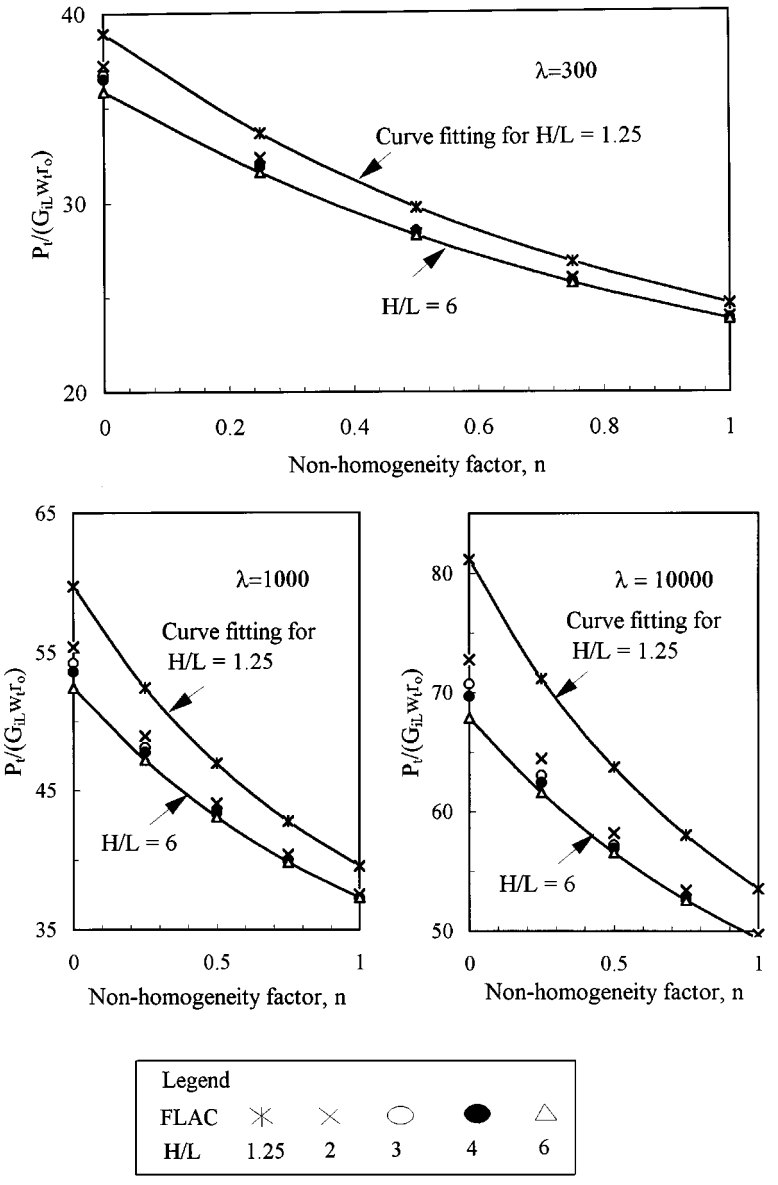

Figure 6. Influence of the H/L on the pile–head stiffness ($L/r_0 = 40$, $v_s = 0{\cdot}4$)

(2) The SA analysis progressively overestimates the stiffness with either increase in non-homogeneity factor n (particularly, $n = 1$), or decrease in pile–soil relative stiffness factor. However, the difference is less than 20 per cent.
(3) For a pile in homogeneous soil ($n = 0$), the CF and SA approaches are exactly the same as illustrated in Appendix II. However, since different value of A have been adopted, the two approaches predict slightly different values of the head stiffness.

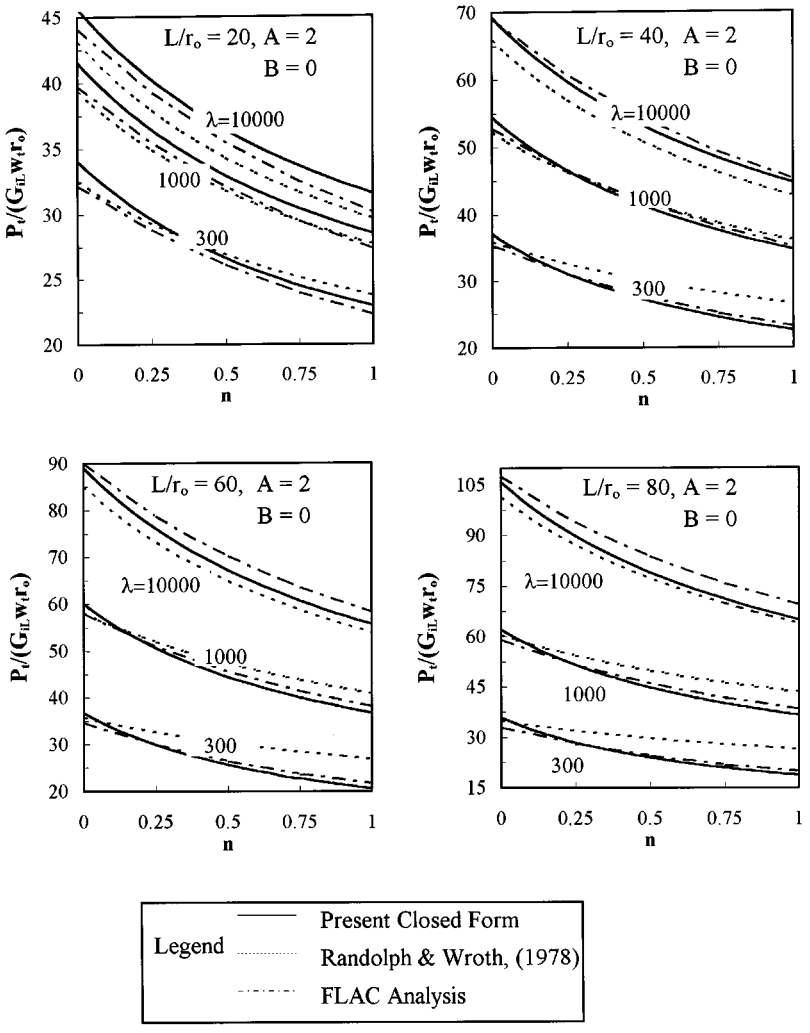

Figure 7. Comparison of pile–head stiffness by FLAC, SA ($A = 2{\cdot}5$) and CF ($A = 2$) analyses

The ratio of pile head and base settlement estimated by equation (25) has been compared with those from the FLAC analyses in Figure 8. For extremely compressible piles, the CF solutions diverge from the FLAC results, probably because the displacement prediction becomes progressively more sensitive to the neglecting of the interactions between each horizontal layer of soil.

Load settlement

The load-settlement relationship furnished by equations (32) and (33) will be verified by continuum-based analyses in this section. Detailed results are compared for a particular set of pile and soil parameters, concentrating on the elastic–plastic response of the pile.

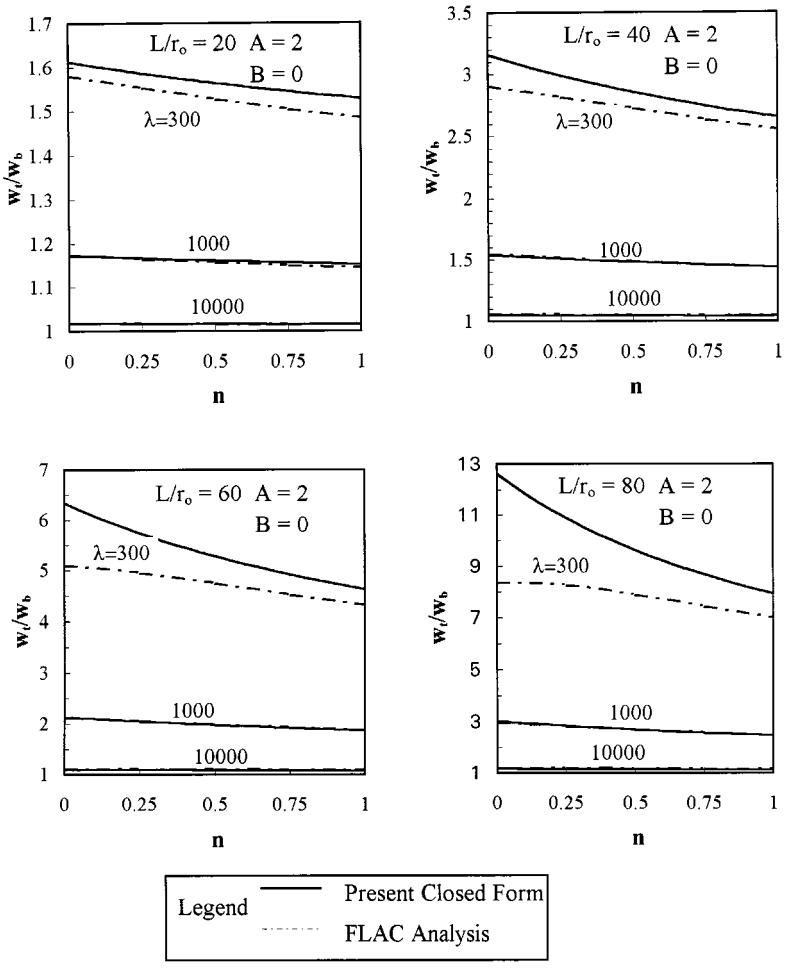

Figure 8. Comparison between the ratio of head settlement and base settlement by FLAC analysis and the CF solution

Homogeneous case. A pile of 30 m in length, and 0·75 m in diameter, is located in a homogeneous soil layer 50 m deep. The initial tangent modulus of the soil (for very low strains) is 1056 MPa, Poisson's ratio is taken as 0·49, and a constant limiting shaft resistance of 0·22 MPa is adopted over the pile-embedded depth. The Young's modulus of the pile is taken as 30 GPa. The numerical analyses by GASPILE and the closed-form solutions for the load-settlement curves are shown in Figure 9, together with the results from a finite element analysis involving the use of a non-linear soil model,[19] and from two kinds of boundary element analyses utilizing an elastic–plastic continuum-based interface model and a hyperbolic continuum-based interface model, respectively.[18] The results demonstrate that the load transfer analysis is very consistent with other approaches. However, as noted by Poulos,[18] the response of very stiff piles (e.g. a value of Young's modulus of the pile being 30,000 GPa), obtained using an elastic perfectly plastic soil response, can differ significantly from that obtained using a more gradual non-linear soil model.

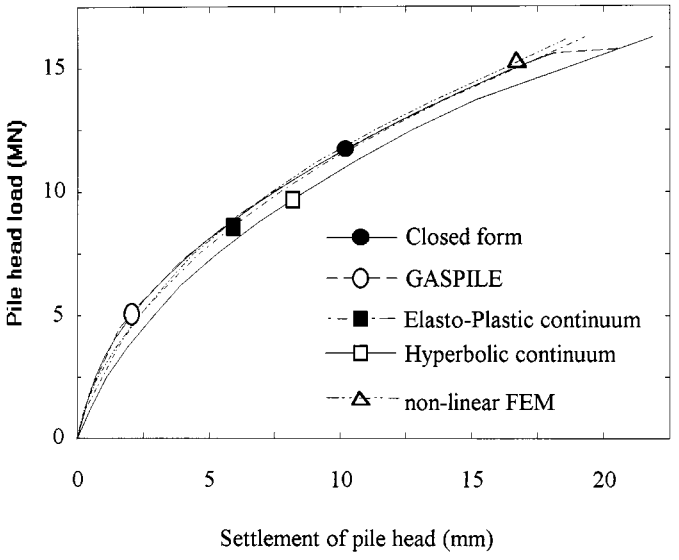

Figure 9. Comparison between various analyses of single–pile load–settlement behaviour

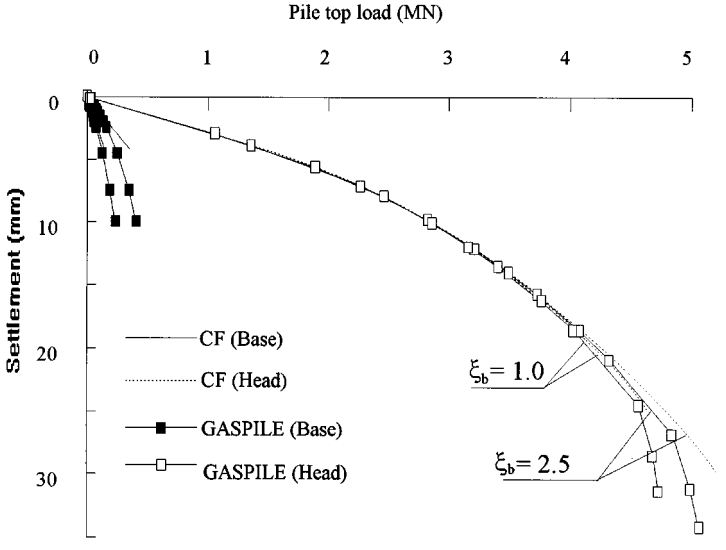

Figure 10. Effect of base end-bearing factor on P–S response

Generally speaking, except for short piles, the pile-head response is only slightly influenced by base shear behaviour, as shown in Figure 10 for two end-bearing factors of $\xi_b = 1$ and 2·5. The non-linear base behaviour, as illustrated by the difference between the non-linear GASPILE and linear (closed-form) analyses, will become obvious only when local shaft displacement at the base level exceeds the limiting displacement, w_e.

Non-homogeneous case. Previous analyses[10,20,21] have reported that pile-head stiffness substantially decreases as the soil shear modulus non-homogeneity factor (n) increases. This is partly because the modulus at the pile tip level was kept constant. Therefore, as n increases, the average shear modulus over the pile length decreases (see equation (2)). To explore the effect of the distribution alone, when the non-homogeneity factor ($\theta = n$) is changed, the average shaft shear modulus should be kept as a constant and also all the other parameters be identical. In such a way, the closed-form prediction by $\psi_0 = 0$ (linear elastic–plastic case) has been shown in Figure 11(a). In this particular case, only about 30 per cent difference due to variation in the n is noted within the elastic stage. Both the pile-head load and settlement, at which slip is initiated, decreases as n increases, as demonstrated in Figures 11(b) and 11(c). It should be noted that since

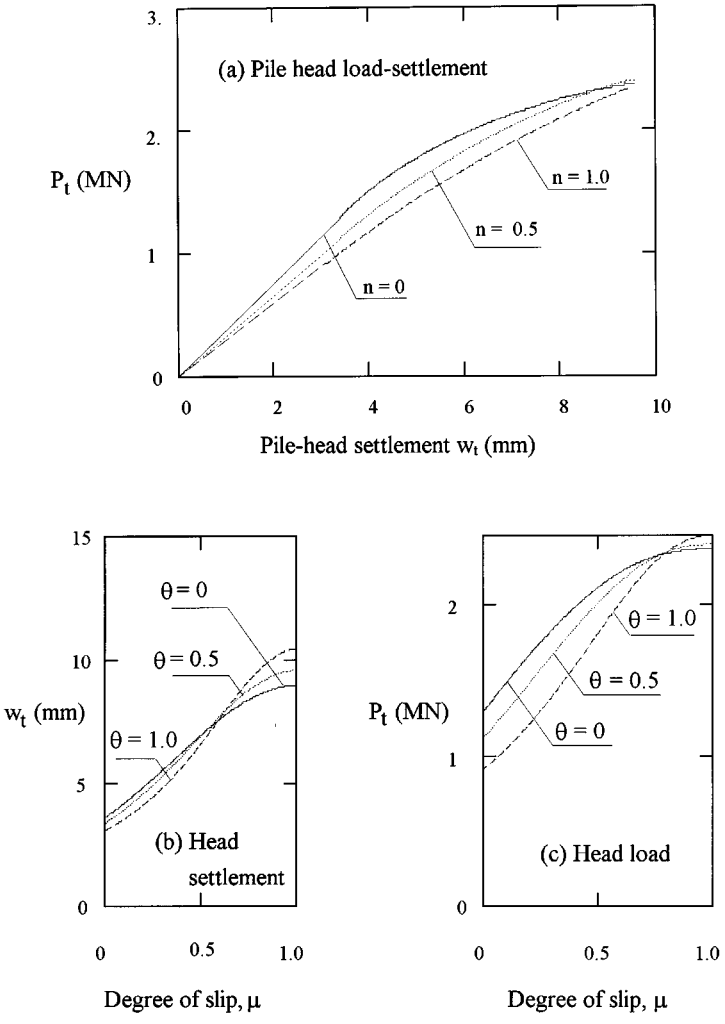

Figure 11. Effect of slip development on pile–head response ($n = \theta$)

the average shaft friction is identical in all three cases, the curves converge towards a similar value of pile head load as full slip develops ($\mu \to 1$). The small variation in pile head load at full slip is due to difference in base load.

SETTLEMENT INFLUENCE FACTOR

The above analysis is further substantiated for different slenderness ratio and relative pile–soil stiffness cases.

Settlement influence factor

The settlement influence factor, I, is defined as the inverse of a pile-head stiffness; therefore,

$$I = \frac{G_{iL} w_t r_0}{P_t} \tag{36}$$

where I is the settlement influence factor. While within the elastic stage, the factor can be derived directly from equation (28)

$$I = \frac{1}{\pi\sqrt{2}C_{vo}} \sqrt{\frac{\zeta}{\lambda}} \tag{37}$$

It is also straightforward to obtain an elastic–plastic formula for the factor, in terms of equations (32) and (33). The settlement influence factor is mainly affected by pile slenderness ratio, pile–soil relative stiffness factor, the degree of the non-homogeneity of the soil profile and the degree of pile–soil relative slip.

Pile slenderness ratio influence

Figure 12 shows the settlement influence factor for a pile of different slenderness ratios in a Gibson soil, at a constant relative stiffness factor ($\lambda = 3000$), together with the BEM analysis based on Mindlin's solution,[18] BEM analysis of three-dimensional solids,[20] and the approximate closed-form solution by Randolph and Wroth.[7] The effect of slenderness ratio on the settlement influence factor reflected by the closed-form solution is generally consistent with those provided by the other approaches.

Pile–soil relative stiffness effect

Using identical values as mentioned previously, the settlement influence factor, I, was estimated by equation (37) for a list of given λ, which are shown in Figure 13 for four different slenderness ratios for $n = 0$ and 1, in comparison with the boundary element (BEM) analysis by Poulos[10] and the current FLAC analysis. The BEM analysis is for the case of $H/L = 2$, while this CF solution corresponds to the case of $H/L = 4$. As presented early in Figure 4, increase in the value of H/L can lead to decrease in pile-head stiffness and thus an increase in the settlement influence factor. For the case of $L/r_0 = 50$, $\lambda = 26{,}000$ ($K_b = 10{,}000$), $n = 0$, an increase in H/L from 2 to infinity can lead to an increase in the settlement factor by up to 21 per cent.[10] In view of the H/L effect, the closed-form solutions are generally quite consistent with the numerical analysis.

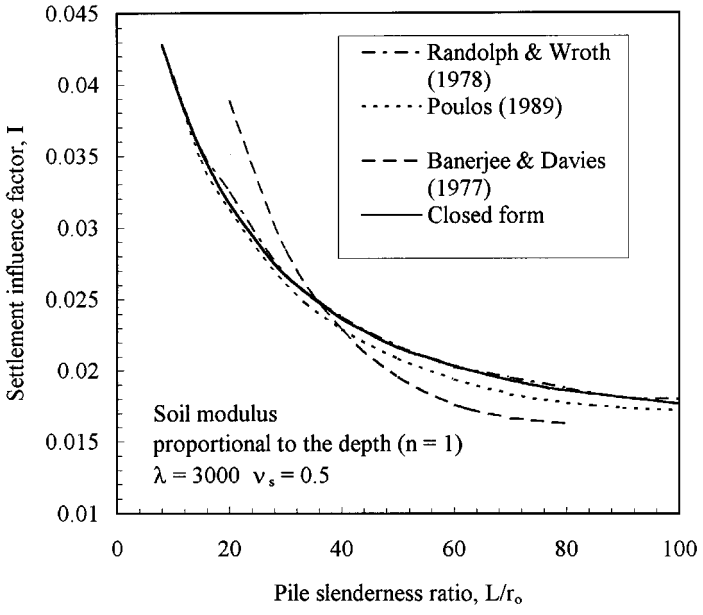

Figure 12. Comparison of the settlement influence factor by various approaches

CASE STUDY

The non-homogeneous soil property and the pile–soil relative slip can be readily taken into account by the established solutions. An example analysis is demonstrated as follows. The test reported by Gurtowski and Wu[22] describes the detailed measured response of a pile. The pile was 0·61 m wide octagonal prestressed concrete hollow pile with a plug at the base, and was driven to a depth of about 30 m. For the current analysis, the parameters used by Poulos[18] have been adopted directly as shown below: Young's modulus of the pile was 35 GPa; soil Young's modulus is approximated by 4 N MPa (N = SPT value); N increases almost linearly with depth from 0 at ground surface to 70 at a depth of 30 m. The limiting shaft stress is taken as 2 N kPa, the base-limiting stress is 0·4 MPa, and the soil Poisson's ratio is 0·3. The pile-head and base load-settlement predictions by GASPILE with $R_{fs} = 0{\cdot}9$, $G_i/\tau_f = 769{\cdot}2$, $R_{fb} = 0{\cdot}9$ and by the closed-form solutions with $\psi_0 = 0{\cdot}5$ are shown in Figure 14 together with those predicted by boundary element analysis.[18] Good comparisons have been demonstrated between the current predictions and the measured results, except at failure load levels. The divergence at high load between the current predictions and those of Poulos[18] is because the ultimate base stress of 0·4 MPa assumed in the current GASPILE and closed-form analyses is different from that used in Poulos' boundary element analysis.

Load–displacement distribution down a pile

Load and displacement distribution below and above the transition depth may be estimated in terms of the elastic and elastic–plastic solutions. Under a given pile-head load, the depth of the

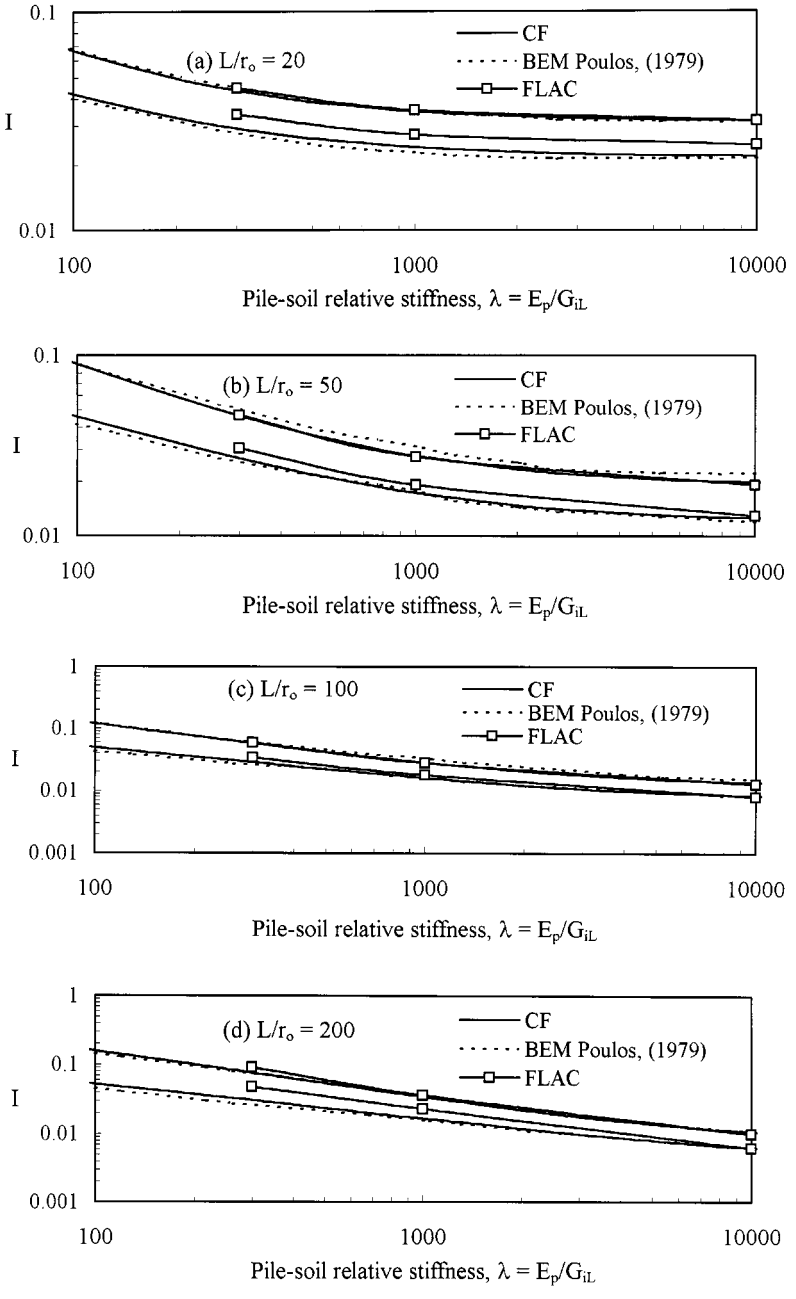

Figure 13. Comparison of settlement influence factor from different approaches

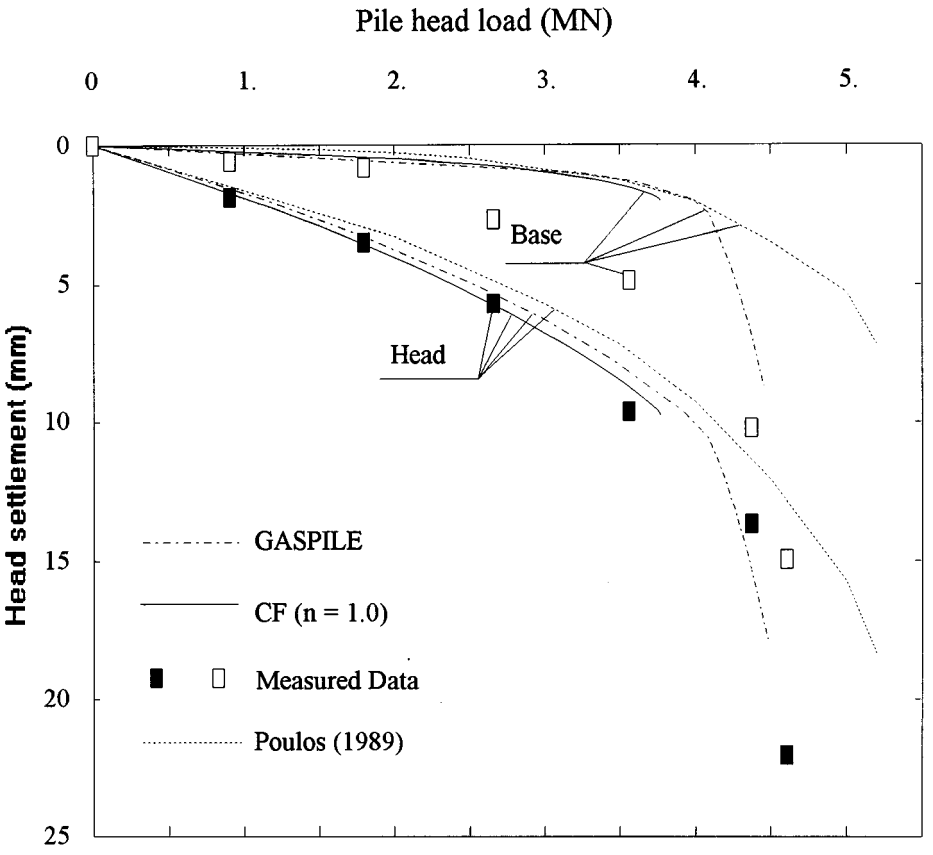

Figure 14. Comparison among different predictions for load settlement (measured data from Reference 22)

transition is expressed by the degree of slip, and can be estimated by equation (32) (i.e. by using Mathcad™), which is also affected by the non-homogeneity factor n. At a depth below the transition point, the local shaft displacement must be less than the limit displacement, w_e. Therefore, the distribution may be estimated by equations (25) and (26), respectively. Otherwise, with an estimated μ, the distribution of load and displacement within the upper plastic zone can be evaluated by equations (34) and (35) displacement within the upper plastic zone can be evaluated by equations (34) and (35), respectively. If a pile–head load exceeds the load corresponding to the full shaft slip, then the difference should be attributed to the base load.

For this typical example, the degrees of slip, μ at $P_t = 1{\cdot}8$ MN are 0·058, 0·136, 0·202, 0·258 and 0·305 for $n = 0$, 0·25, 0·5, 0·75, and 1·0, respectively. For $P_t = 3{\cdot}45$ MN, $\mu = 0{\cdot}698$, 0·723, 0·743, 0·758, 0·771 correspondingly. For $P_t = 4{\cdot}52$ MN, full shaft slip is expected at any value of n, and the base should take a load of 1·07 MN. The closed-form predictions of load and displacement distributions down the pile are generally consistent with those from non-linear GASPILE analysis. For the three different soil profiles of $n = 0$, 0·5 and 1·0, the settlement (only at two load levels, $P_t = 1{\cdot}8$ and 3·45 MN) and load transfer are shown in Figure 15 together with the those from GASPILE. A summary of the closed-form solutions and that from GASPILE ($n = 1$ case only)

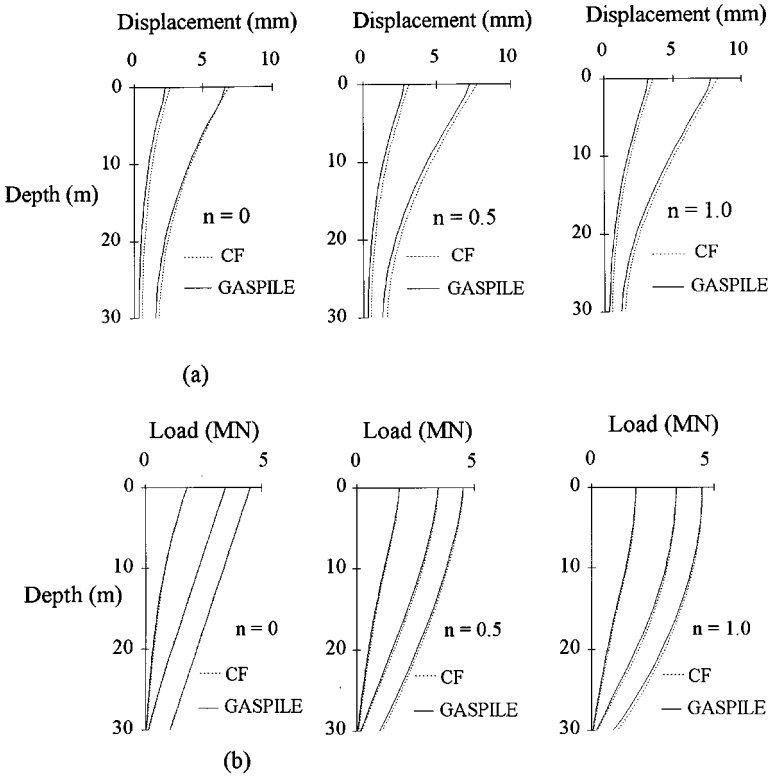

Figure 15. Comparison between the CF and the non-linear GASPILE analyses (case study): (a) down pile displacement distribution; (b) down pile load distribution

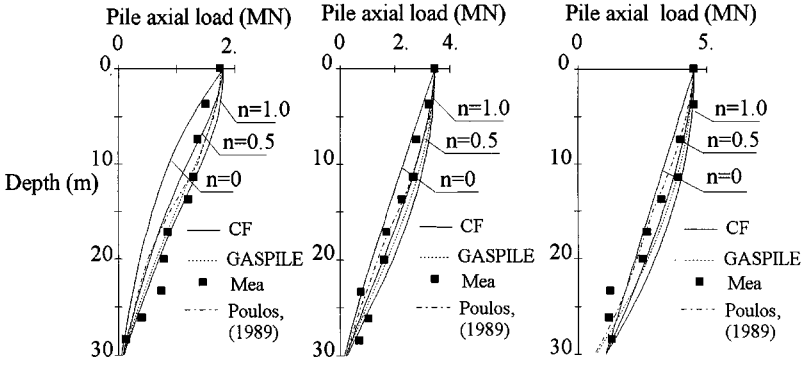

Figure 16. Comparison among different predictions of the load distribution

are shown in Figures 16(a)–(c) in conjunction with those by Poulos[18] and the measured data. The results show that the linear correlations of the soil strength and shear modulus with the values of SPT ($n = 1$) yield reasonable predictions of the pile response in comparison with the measured.

CONCLUSION

The analysis outlined in this paper has attempted to provide a more rigorous approach to the analysis of a pile in a non-homogenous soil medium. The accuracy of the solutions based on the load transfer approach is very good compared with those from continuum and non-linear load transfer analyses.

The following conclusions can be drawn:

(1) A non-linear elastic–plastic analysis makes only a slight difference from that of the simplified linear elastic–plastic analysis. Therefore, the newly established closed-form solutions based on the simplified elastic–plastic soil response are sufficiently accurate even for estimation of the non-linear response.
(2) The previously reported significant influence of n on pile–head stiffness or settlement influence factor is partly caused by the alteration of average shear modulus over the pile length, and partly by the distribution. For a constant average shear modulus, the influence of the n on the pile–head stiffness becomes relatively minor.
(3) The effect of the pile–soil relative slip on estimating load-settlement behaviour including the load and displacement distributions down the pile can be readily simulated by the newly established theory.

From the second conclusion, it may be inferred that even for a complicated shear modulus profile, the non-homogeneity factor, n, may be adjusted to fit the general trend of the modulus with depth. The solution presented here may thus still be applied with reasonable accuracy.

ACKNOWLEDGEMENTS

The first author is currently supported by an Australian Overseas Postgraduate Research Scholarship and by scholarship and by scholarships from the University of Western Australia. This financial assistance is gratefully acknowledged.

APPENDIX I

Notation

A	constant for estimating the ζ
A_g	constant for soil shear modulus distribution
A_p	cross-sectional area of pile
B	constant for estimating the ζ
C_{vo}	value of $C_v(z)$, as z approaches zero
E_p	elastic modulus of pile body
E_{iL}	Young's modulus of soil at pile base level
G_{ave}	average soil shear modulus over the entire pile-embedded depth
G_i	initial soil shear modulus
G_{ib}	initial shear modulus at just beneath pile base level

G_{iL} initial shaft soil shear modulus at just above the pile base level
I settlement influence factor
k_s a factor representing pile–soil relative stiffness
L embedded pile length
L_1 the depth of transition from elastic to plastic phase
L_2 length of the elastic part of the pile under a given load
n power of the shear modulus distribution, non-homogeneity factor
P_b axial force of pile body at a pile base
$P(z)$ axial force of pile body at depth z
P_e axial load at the depth of transition (L_1) from elastic to plastic phase
P_{fb} ultimate base load
P_t load acting on pile head
R_{fb} hyperbolic curve-fitting constant for pile base load–settlement curve
R_{fs} ratio of limiting and ultimate shaft shear stress
r_0 pile radius
r_m radius of zone of shaft shear influence
$u(z)$ axial pile displacement at a depth of z
w_b settlement of pile base
w_e limiting elastic shaft displacement calculated by using τ_{max} in the equation
w_t pile-head settlement
$w(z)$ pile–soil relative displacement at depth z for a given time
β non-dimensional shaft stiffness factor for the case of $n = 0$
ζ measured influence of load transfer
η homogeneity factor by Poulos
K_b relative pile–soil stiffness ratio between pile Young's modulus and the initial soil Young's modulus at just above the base level (E_p/E_{iL})
λ relative stiffness ratio between pile Young's modulus and the initial soil shear modulus at just above the base level (E_p/G_{iL})
θ power of the depth for shaft limit stress distribution
A_v constant for shaft limit stress distribution
μ degree of pile–soil relative slip
ν_s Poisson's ratio of soil
ξ_b end-bearing shear modulus non-homogeneous factor (G_{iL}/G_{ib})
ρ_g ratio of the average soil shear moduli to G_{iL}
τ_f limiting local shaft stress
τ_o shear stress on pile–soil interface
τ_{ult} ultimate local shaft stress
ψ_0 non-linear factor ($\tau_o R_f/\tau_f$), stress level
ω base factor accounting for effect of the pile-embedded depth and the base shape

APPENDIX II

Vertical piles in homogeneous soil

This appendix shows that the solutions for a pile in a homogeneous soil published previously can be achieved readily from the new theory established in the paper.

Elastic solution. For a pile in an ideal non-linear homogenous soil subject to vertical loading, since $n = 0$, the coefficients in equation (27) can be simplified as

$$C_1(z) = C_4(z) = \frac{1}{k_s L}\sqrt{\frac{L}{z}}\sinh k_s(L - z)$$
$$C_2(z) = C_3(z) = \frac{1}{k_s L}\sqrt{\frac{L}{z}}\cosh k_s(L - z) \tag{38}$$

Shaft displacement, $w(z)$, and axial load, $P(z)$, of the pile body at depth of z are expressed as

$$w(z) = w_b(\cosh k_s(L - z) + \chi_v \sinh k_s(L - z)) \tag{39}$$

$$P(z) = k_s E_p A_p w_b(\chi_v \cosh k_s(L - z) + \sinh k_s(L - z)) \tag{40}$$

where $E_p A_p$ is the cross-sectional rigidity of an equivalent solid cylinder pile. Supposing the load acting on the pile head is P_t, thereby a clear understanding of the relationship among the force on a pile base and head, the base settlement, w_b and the shaft (base) settlement ratio can be established by equation (40)

$$P_b \cosh \beta + k_s E_p A_p w_b \sinh \beta = P_t \tag{41}$$

At the head of a pile ($z = 0$), from equation (39), the settlement w_t can be expressed as

$$w_t = w_b(\cosh \beta + \chi_v \sinh \beta) \tag{42}$$

where $\beta = k_s L$. With equation (28), the non-dimensional relationship between the head load P_t (hence deformation, w_p) and settlement w_t is derived as

$$\frac{w_p}{w_t} = \beta(\tanh \beta + \chi_v)/(\chi_v \tanh \beta + 1) \tag{43}$$

where $w_p = P_t L/(E_p A_p)$. Equation (43) can be expanded to that given by Randolph and Wroth,[7] in which β is equal to the 'μL' shown in their paper and χ_v should be replaced by equation (24).

Elastic–plastic solution. Within the elastic–plastic stage, in terms of equations (43), and (11), the pile load at the transition depth is easily derived

$$P_e = \frac{\pi d \tau_f L}{\beta}\left(\frac{\tanh \bar{\beta} + \chi_v}{\chi_v \tanh \bar{\beta} + 1}\right) \tag{44}$$

where $\bar{\beta} = k_s L_2 = \beta(1 - \mu)$; for plastic zone ($0 \leqslant z \leqslant L_1$). Considering equations (30) and (44), it follows that

$$P_t = \pi d \tau_f L\left(\mu + \frac{1}{\beta}\frac{\tanh \bar{\beta} + \chi_v}{\chi_v \tanh \bar{\beta} + 1}\right) \tag{45}$$

In terms of equating (33) and (11), the pile–head settlement can also be written as

$$w_t = w_e\left(1 + \frac{\beta^2 \mu^2}{2} + \beta\mu \frac{\tanh \bar{\beta} + \chi_v}{\chi_v \tanh \bar{\beta} + 1}\right) \tag{46}$$

REFERENCES

1. H. M. Coyle and L. C. Reese, 'Load transfer for axially loaded piles in clay', *J. Soil Mech. Found. Eng. Div.*, **92**(2), 1–26 (1966).
2. Y. K. Chow, 'Discrete element analysis of settlement of pile groups', *Comput. struct.*, **24**(1), 157–166 (1986).
3. P. Clancy and M. F. Randolph, 'An approximate analysis procedure for piled raft foundations, *Int. j. numer. analyt. methods geomech.*, **17,** 849–869 (1993).
4. J. D. Murff, 'Response of axially loaded piles', *J. Geotech. Eng. Div. ASCE*, **101,** 357–360 (1975).
5. J K. Kodikara and I. W. Johnston, 'Analysis of compressible axially loaded piles in rock', *Int. j. numer. analyt. methods geomech.*, **12,** 427–437 (1994).
6. E. Motta, 'Approximate elastic–plastic solution for axially loaded piles', *J. Geotech. Eng. Div. ASCE*, **120,** 1616–1624 (1994).
7. M. F. Randolph and C. P. Wroth, 'Analysis of deformation of vertically loaded piles', *J. Geotech. Eng. Div. ASCE*, **104,** 1465–1488 (1978).
8. *Itasca* "*FLAC—Users' Manual*", Itasca Consulting Group, Minneapolis, 1992.
9. J. R. Booker, N. Balaam and E. H. Davis, 'The behaviour of an elastic non-homogeneous half-space, Parts I & II', *Int. j. numer. analyt. methods geomech.*, **9,** 353–367, 369–381 (1985).
10. H. G. Poulos, 'Settlement of single piles in nonhomogeneous soil', *J. Geotech. Eng. Div. ASCE*, **105,** 627–642 (1979).
11. W. D. Guo, 'Analytical and numerical analyses of pile foundations', *Ph.D thesis*, The University of Western Australia, 1997.
12. M. F. Randolph, 'A theoretical study of the performance of pile', Thesis, Cambridge University, at Cambridge, England, 1977.
13. L. M. Kraft, R. P. Ray and T. Kagawa, 'Theoretical t–z curves', *J. Geotech. Eng. Div. ASCE*, **107,** 1543–1561 (1981).
14. W. D. Guo and M. F. Randolph, 'Settlement of pile groups in non-homogeneous soil', *Proc. 7th ANZ Conf. on Geomechnics*, Vol. 1, 1996, pp. 631–636.
15. T. Whitaker and R. W. Cooke, 'An investigation of the shaft and base resistance of large bored piles in London clay', in *Large Bored Piles*, Institution of Civil Engineers, London, 1996, pp. 7–50.
16. S. Armaleh and C. S. Desai, 'Load deformation response of axially loaded piles', *J. Geotech. Eng. Div. ASCE* **113,** 1483–1499 (1987).
17. M. F. Randolph, RATZ, *Load Transfer Analysis of Axially Loaded Piles*, Dept. of Civil Engrg. The University of Western Australia, 1986.
18. H. G. Poulos, 'Pile behaviour-theory and application', *Rankine Lecture*, *Geotechnique*, **39**(3), 365–415 (1989).
19. R. J. Jardine, D. M. Potts, A. B. Fourie and J. B. Burland, 'Studies of the influence of non-linear stress–strain characteristics in soil–structure interaction', Geotechnique, **36,** 377–396 (1986).
20. P. K. Banerjee and T. G. Davies, 'Analysis of pile groups embedded in Gibson soil', *Proc. 9th Int. Conf. on Soil Mech. and Found. Engrg.*, Tokyo, Japan, Vol. 1, 1977, pp. 381–386.
21. R. K. N. D. Rajapakse, 'Response of axially loaded elastic pile in a Gibson soil', Geotechnique, **40,** 237–249 (1990).
22. T. M. Gurtowski and M. J. Wu, 'Compression load tests on concrete piles in alluvium', in J. R. Meyer (ed) *Anal. Design of Pile Foundations*, Am. Soc. Civ. Engrs., 1984, pp. 138–153.

